DRYING OF MOCK SPENT NUCLEAR FUEL ELEMENTS

John C. Crepeau[1], Stephen Reese[1], Hugh M. McIlroy, Jr.[1], and Rebecca E. Lords[2]

[1]Department of Mechanical Engineering, University of Idaho,
P.O. Box 50778, Idaho Falls, Idaho 83405, USA

[2]Lockheed Martin Idaho Technologies Company
P.O. Box 1625, Idaho Falls, Idaho 83415-3114, USA

ABSTRACT

Spent nuclear fuel elements are stored in underwater cooling pools until the elements can be safely handled and prepared for interim dry storage. The fuel was intended for short-term storage in water before it was to be reprocessed. However, the fuel will no longer be reprocessed, and extended storage in water has caused many of the aluminum-clad elements to degrade, exposing the uranium fuel. In addition, sludge, comprised of corroded aluminum and sediment, has accumulated in and around the fuel plates. The water in the sludge must be removed before the spent fuel elements can be placed in dry storage. Experiments have been performed on mock spent fuel elements with simulated corrosion product applied between the plates. A series of vacuum and heating cycles were used to dry the elements, and a mixture of clay and aluminum oxide was used to simulate corrosion products on the elements.

The procedures used in the experiments were determined to be adequate to dry the mock spent fuel elements, and the temperature behavior of the simulated corrosion product within the fuel elements could be used to determine when the element was dry. On plates where areas of wet simulant were found, a sharp

drying front was observed that separated the wet and dry parts of the simulated corrosion product. The drying front propagated inward towards the center of the mock fuel elements over time.

INTRODUCTION

When a nuclear fuel element reaches the end of its useful life, it is commonly removed from the reactor core and placed in underwater storage pools. Pool water provides radiation shielding and allows thermal cooling of the spent elements.

At the Idaho National Engineering and Environmental Laboratory (INEEL), a number of aluminum-clad plate fuel elements have been underwater for decades. During this time, the aluminum cladding has corroded on many of the elements, exposing the nuclear fuel. Airborne dust particles have entered the storage pools, creating a clay-like sludge that has settled between the fuel plates and on the elements. Most of these spent fuel elements were intended to be stored underwater for a short period prior to reprocessing. Since reprocessing has been discontinued, the time has come to remove the spent fuel from the pools and prepare them for dry storage. However, the corroded aluminum cladding and sludge accumulations have presented difficulties in drying the spent fuel.

Before the elements can be placed in storage, they must be free of any physically bound water. Residual moisture must be removed from the elements to avoid additional degradation of the aluminum cladding, and to prevent possible build-up of excess pressure if placed within a sealed storage system (Lords et al, 1996). These issues, and fuel handling considerations, limit the methods that can be used to dry the spent fuel elements. The INEEL has chosen to use a combination of vacuum drying (Glang, 1970) and heating to remove the free water from the spent fuel corrosion product.

Experiments have been performed on mock fuel elements using simulated corrosion products to test the INEEL drying protocol and verify that the procedures dry the mock fuel elements. A thermogravimetric analyzer was used to determine the level of dryness of the simulated corrosion product. This effort also

supports the recommendations (Kasakura and Hasatani, 1996; Itaya and Hasatani, 1996) for further studies in drying industrial materials.

EXPERIMENTAL APPARATUS

The drying chamber used in the experiments is a half-scale mock-up of the actual drying station. The chamber is constructed of 18 inch diameter, schedule 40, 304 stainless steel pipe, and is 57 inches tall. The chamber has a quartz window through which one can observe the experiment, and an instrumentation panel port which serves as a feedthrough for the interior thermocouples.

The chamber is connected to a Leybold Sogevac rotary vane vacuum pump, through a High Efficiency Particulate Air (HEPA) filter, and isolation valves. Surrounding the chamber are three, 3.5kW band heaters which are connected to a PID controller, allowing for precise temperature control. The drying system is monitored and controlled in real-time by an HP3852A Data Acquisition System and an Apple Macintosh Quadra 650 running LabVIEW experiment interface software. A schematic of the system is displayed in Figure 1, and a photo of the drying chamber with its associated components is shown in Figure 2.

The tests were performed on aluminum plates, which represented the spent fuel elements, and selected tests were performed on mock advanced test reactor (ATR) fuel elements. Single and multiple short elements (30.5 cm long) and single and multiple long elements (121.9 cm long) were used in the experiments. Figure 3 shows a mock ATR fuel element, and Figure 4 is an end view of the aluminum plates.

Besides corrosion of the aluminum cladding, airborne dust and silt is blown into the storage facility from the surrounding area. This sediment drifts into open cooling channels in the fuel, forming a mixed deposit of sediment and aluminum oxide. Observation of the storage environment and pool sludge at the INEEL has indicated that the actual sludge which accumulates on the plate fuel will be a combination of components (Anderson, 1995).
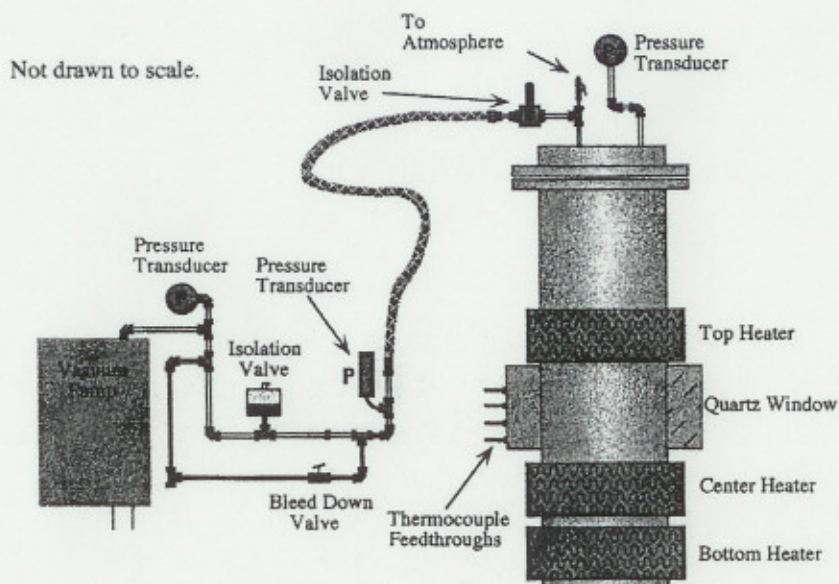
Figure 1. Schematic of the experimental drying apparatus.

A mixture of clays (bentonite and kaolinite), aluminum oxide (boehmite), and water was determined to be an appropriate representation of the actual deposit expected in the plate fuels. This mixture was developed to simulate the chemistry and particle size of local soils (Nace et al., 1956) with measured amounts of boehmite added. The boehmite powder ($Al_2O_3 \cdot 1.3H_2O$) is used to model the aluminum corrosion product. Table 1 shows the percent by weight of the materials used in the simulated corrosion product mixture. The water is blended with the dry mixture to achieve a thin putty. This putty is spread between the plates of the mock fuel elements at a constant thickness. There was good adhesion between the simulant and aluminum plates, preventing accumulation of simulant on the bottom of the chamber. Figure 5 shows how the simulated corrosion product is applied to the aluminum plates. The elements are then subjected to a drying protocol of prescribed temperature ranges, heating rates, and pressure levels. This protocol was defined for fuel safety and handling considerations.
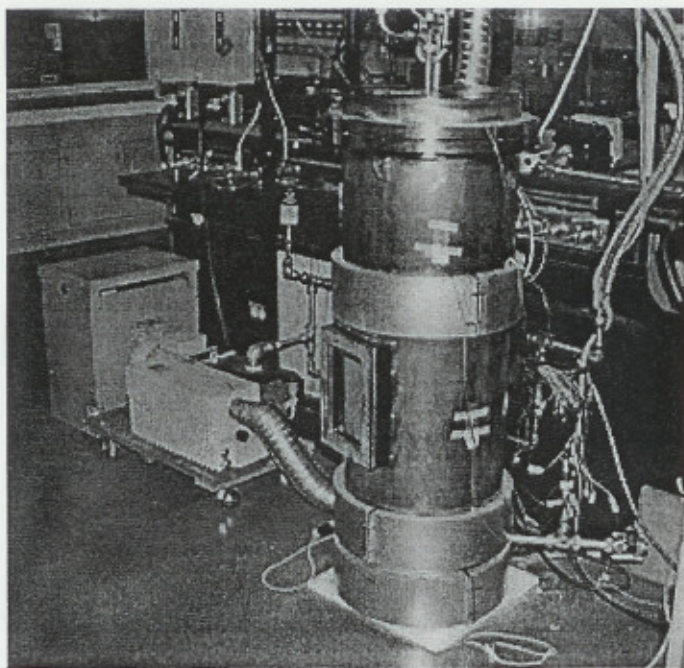
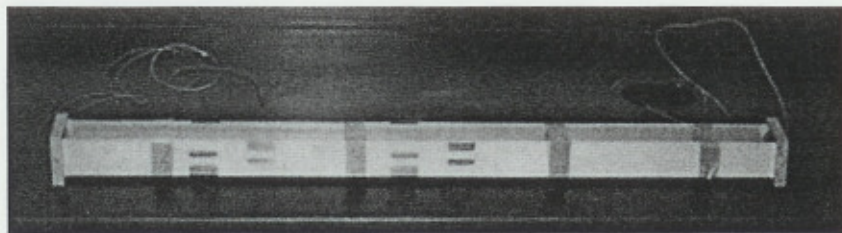Figure 2. Photo of the experimental drying apparatus.

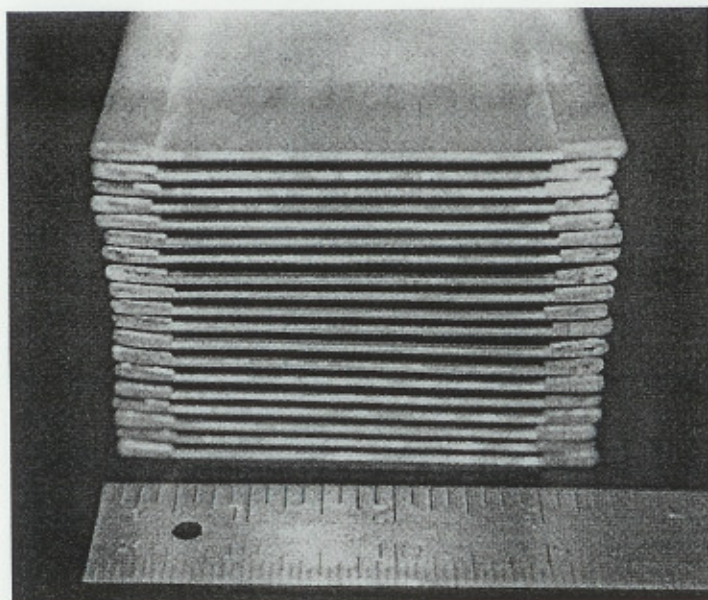Figure 3. Mock fuel element with thermocouples attached.

Figure 4. End view of the plates used in the drying experiments. The plates represent an aluminum-clad spent fuel element. Simulated corrosion product is applied between the plates, and the unit is placed in a drying chamber.

TABLE 1. Composition of Simulated Corrosion Product.

Material	Percent by Weight	
	Dry	Wet
Bentonite	30.8	8.0
Kaolinite	26.6	6.9
Boehmite	42.6	11.1
Water	--	74.0

The simulated corrosion product on the plates was analyzed before and after each drying test. The instrument used for this analysis was a Perkin-Elmer Model TGS-2 Thermogravimetric Analyzer (TGA). The Model TGS-2 is a complete system for accurately recording the weight loss or gain of a sample as it

Figure 5. Application of simulated corrosion product to the mock aluminum plate fuel elements.

is subjected to a precisely controlled temperature environment. This instrument is connected to a Perkin-Elmer Model DSC-2 Differential Scanning Calorimeter via a Perkin-Elmer Model 3700 Data Station. Program parameter values in every analysis were as follows:

    Final Temperature: 860°C
    Starting Temperature: 10°C
    Heating Rate: 5°C/minute
    Cooling Rate: 80°C/minute

The heating rate of 5°C/minute was deemed low enough to provide sufficient data resolution. The cooling rate had no effect on the TGA results.
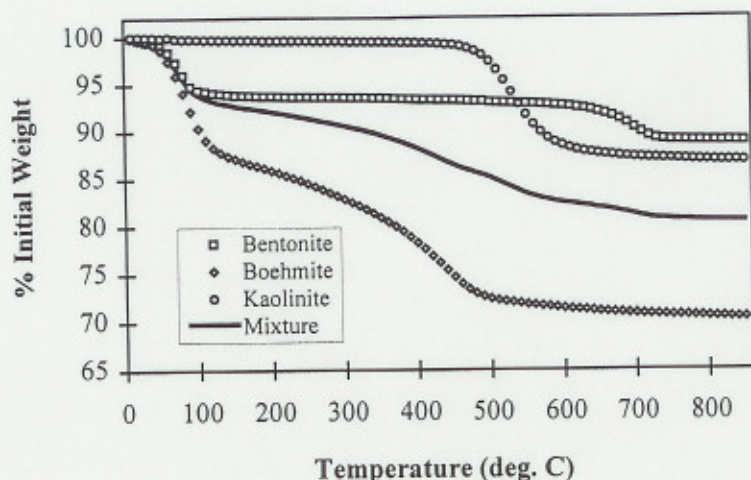
Figure 6. Thermogravimetric analysis of individual constituents of the simulated corrosion product.

RESULTS

Thermogravimetric analysis was performed on each of the dry constituents of the simulated corrosion product: boehmite, bentonite, and kaolinite, in addition to a dry mixture of the components. Figure 6 gives the percentage weight loss for each constituent over temperatures ranging from 10-860°C. Boehmite is the dominant constituent by weight, hence the simulant mixture curve is most similar in shape to the boehmite curve. The effects of the bentonite and kaolinite are clearly noticeable in the latter part of the mixture curve.

The first steep weight change occurs at ~90-100°C on all of the curves except kaolinite. We believe that this indicates the removal of the residual physically absorbed water. Subsequent drops begin around 280, 500, and 680°C, for boehmite, kaolinite, and bentonite, respectively. These changes are consistent with the temperatures corresponding to the removal of waters of hydration for each constituent (Wefers and Misra, 1987).

TABLE 2. Surface Areas of Simulated Aluminum-Clad Plate Fuels

Plate Type	Surface Area (cm^2)
Single Short	3703
Multiple Short	14,813
Single Long	14,813
Multiple Long	59,253

Drying experiments were performed on single and multiple short simulated fuel elements and single and multiple long simulated fuel elements. Table 2 presents the surface areas of these elements. The experiments consisted of a series of vacuum and heating cycles to dry the elements. During the vacuum portion, the drying chamber is evacuated to 5 torr, and held at that pressure for five minutes. This minimum pressure was prescribed by the INEEL protocol to avoid freezing the water within the spent fuel, impeding mass transfer during drying. After the vacuum cycle, the chamber is backfilled with air, and heated with band heaters set at 220°C. This temperature is held for 30 minutes during the first cycle, and for 35, 40, and 45 minutes, respectively, in subsequent cycles.

Because adding significant, unregulated percentages of oxygen to the actual drying chamber could cause reactions with some types of spent nuclear fuel, the drying chamber will be backfilled with an inert gas during the heating process. The temperature and pressure limits of the drying process are stringent, and are fixed at those levels to avoid adverse reactions and additional degradation of the fuel.

A typical plot of the pressure and temperature curves of the interior of a mock fuel element is shown in Figure 7a. The temperature behavior of the thermocouple placed in the center of the middle plate shows when that plate is dry. Since the middle plate is generally the last to dry, it implies dryness of the whole element. For cycles where the center plate is still wet, as the pressure in the
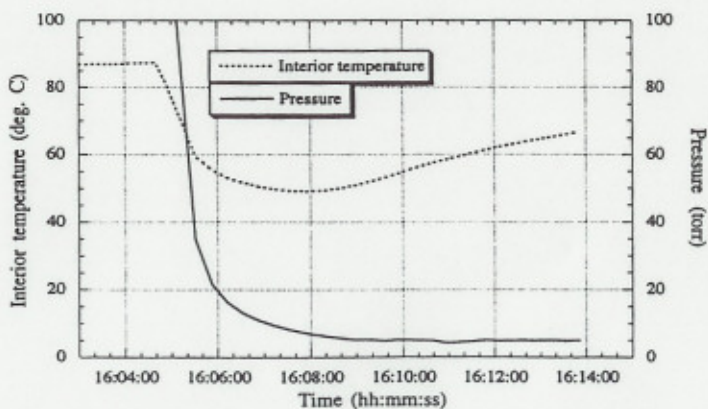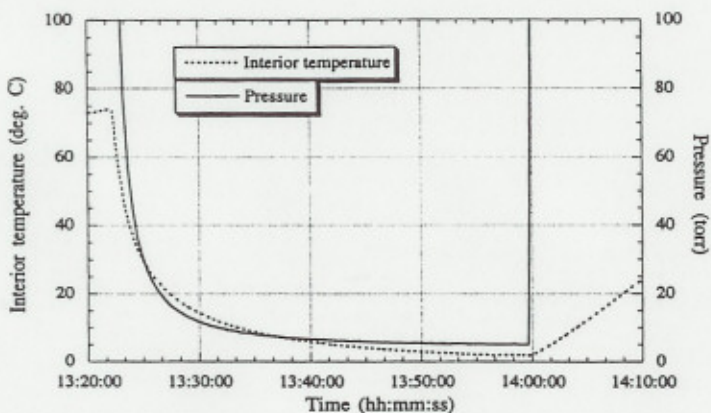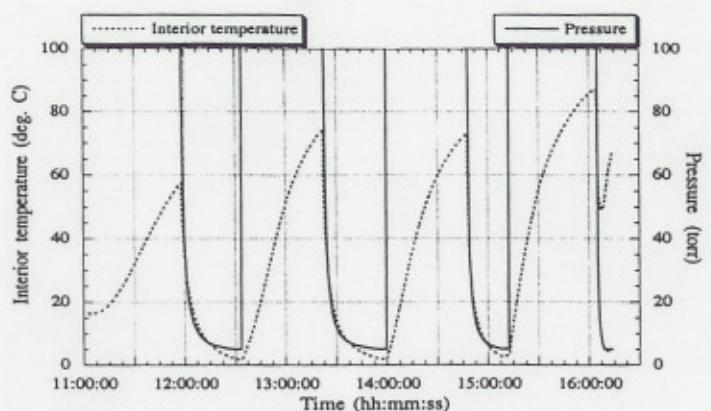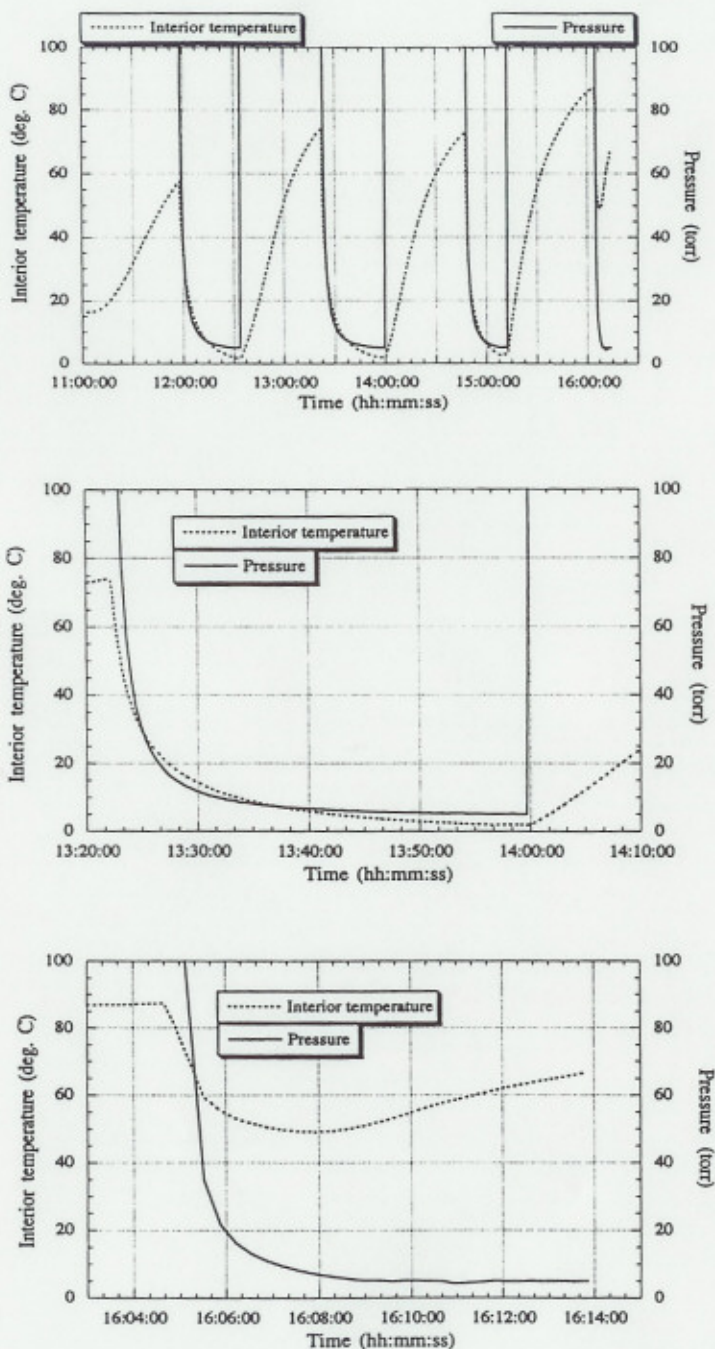
Figure 7. a. Pressure and temperature profile of a typical dry center plate.
         b. Expanded view of the second cycle.
         c. Expanded view of the final cycle.

Figure 7. a. Pressure and temperature profile of a typical dry center plate.
b. Expanded view of the second cycle.
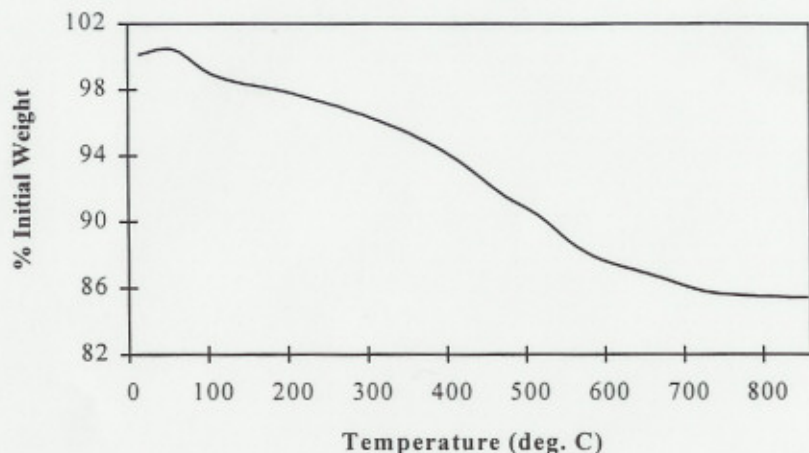c. Expanded view of the final cycle.

Figure 8. TGA curve of a typical dry sample.

chamber reaches 5 torr and is held constant, the temperature stays constant as long as the pressure remains constant. When the center plate is dry, the temperature begins to increase as soon as the pressure ceases to drop and is held constant at 5 torr. During the first three cycles the temperature does not increase while the pressure is held constant at 5 torr. For a close up view of this behavior, see Figure 7b. During the final cycle, the temperature begins to increase as soon as the pressure ceases to drop. Figure 7c shows this behavior.

Using this drying protocol, 72% of the fuel elements were completely dried. The remaining elements had areas of wet simulated corrosion product ranging in size from 4 to 63 cm^2. In these cases, if an additional vacuum/heating cycle was added to the drying procedure, the remaining wet elements could be completely dried. In general, the total drying time increased as more and longer fuel elements were added to the chamber.

After the drying experiment is completed, the elements are removed from the chamber, and samples of the mock corrosion product are taken and placed in the TGA. The TGA results of the dry samples were consistent, and Figure 8 is a

representative TGA curve for such a sample. It shows no steep initial change in weight, as is shown in the mixture curve of Figure 6, implying that the free water has been completely removed during the drying process. Every dried sample experienced a slight increase in weight when initially placed in the TGA. This weight increase indicates that the drying process produces a material that will absorb water from the ambient atmosphere. In other words, the drying process produces a simulated corrosion product that is drier than the ambient.

The average percentage weight loss, as measured by the TGA for the dry samples, was 14.8%. Results of the thermogravimetric analysis established that samples of the wet corrosion product, taken before it has been applied to the plates, lost 76.0% of their weight. Physically bound water makes up 74% of the weight, and 2% is presumed to be chemically bound water. Those samples that lost between 14-20% of their weight in the TGA were declared "dry," whereas samples that lost more than 20% of their weight in the TGA were declared "wet." These data support the visual observations made of the plates upon removal from the drying chamber. The TGA results indicate that although the simulant is drier than the ambient atmosphere, those water molecules which are chemically bound to the simulated corrosion product are not all liberated during the drying process.

Samples were taken from wet spots remaining on a plate element after undergoing the drying process. Figure 9 gives a typical example of the TGA results from a wet sample. The solid line corresponds to a sample of wet corrosion product that had not undergone the drying process (baseline), and the dashed line corresponds to a sample taken from a wet spot that remained on a plate after incomplete drying. Analysis shows that the post drying process simulated corrosion product loses about 60% of its weight by the time it reaches approximately 100°C, and an additional 9% during heating from 100-820°C.

Figures 10 and 11 are photographs of a plate that was completely dried and of a plate with a wet area, respectively. The dry portion of the simulated corrosion product exhibited considerable shrinkage (Ketelaars et al., 1994); nonetheless, it adhered well to the plates.
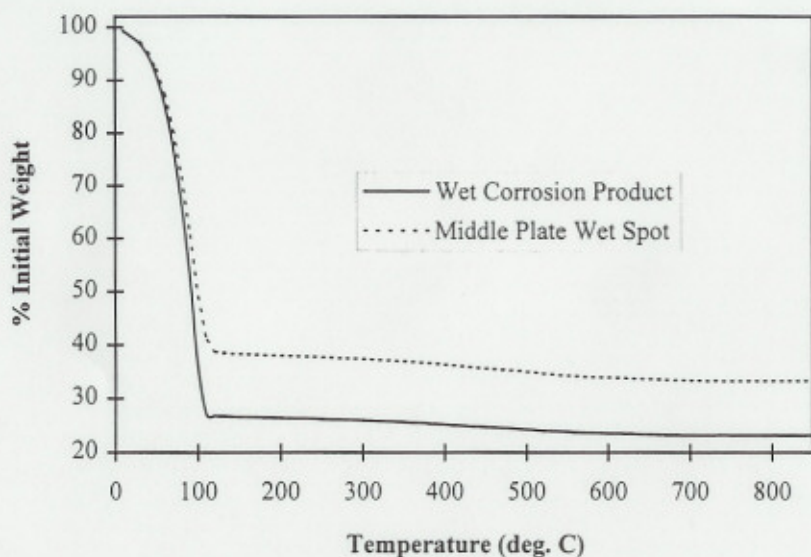
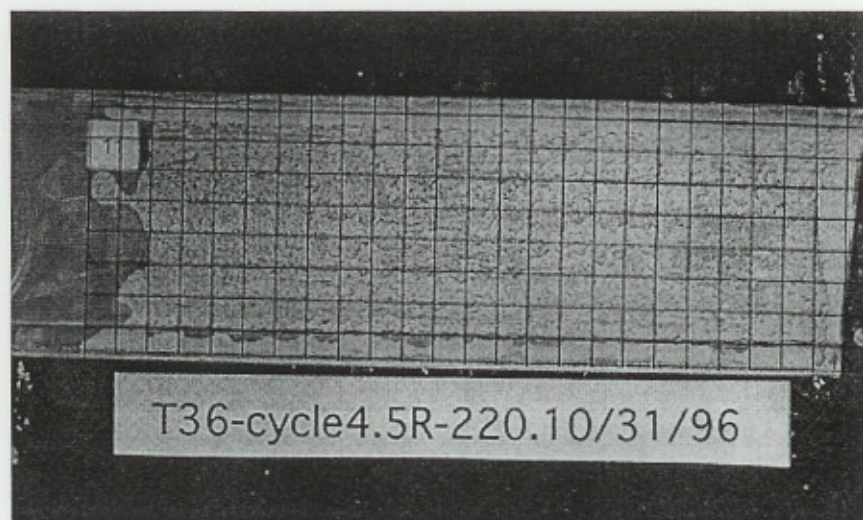Figure 9. TGA curve from a wet sample and a baseline sample.

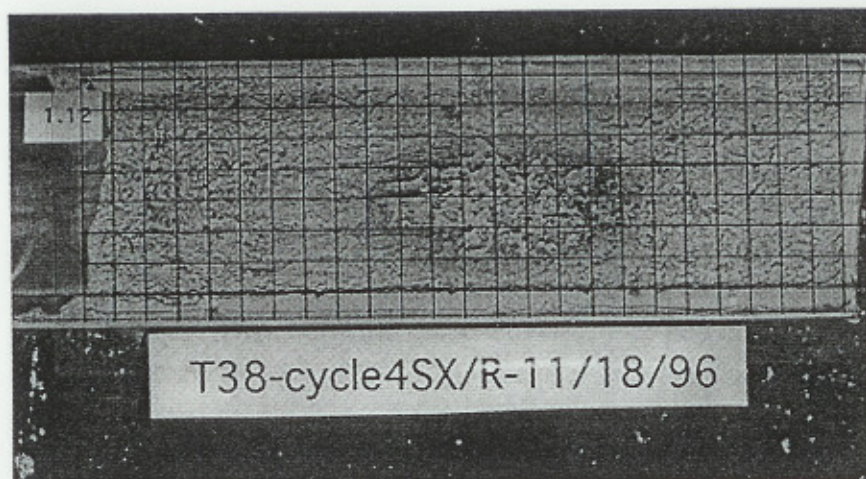Figure 10. Photograph of a dry plate after undergoing the drying process.

Figure 11. Photograph of a plate with a wet spot after undergoing the (incomplete) drying process.

There is an interesting observation concerning the boundary between a wet and dry spot as water is removed from the simulated corrosion product (van der Zanden et al., 1996). Samples were taken near the boundary of a wet spot, on both the dry and wet sides, 10 mm apart. TGA analysis indicated that the dry part was as dry as the rest of the plate, although it was close to the wet boundary. The wet samples were nearly as wet as an undried sample, as shown Figure 9. This disparity indicates that there is a sharp boundary, or receding drying front, between the wet and dry portions of the plate, and that the water does not diffuse gradually through the corrosion product.

The consistency with which the drying process completely dried the elements, and the time required to complete the process, varied widely based on the size and number of elements present (Table 2). The level of dryness of the completely dried plates, however, was very consistent. This fact is supported by the lack of variability in the data taken by the TGA.

The results of the thermogravimetric analysis over the period of research were very consistent and reproducible. Consistent experimental protocols and careful handling of the corrosion product samples reduced the experimental uncertainty. For visually dry samples, the percent weight change ranged from 13.52% to 16.96%, a 3.44% span.

CONCLUSIONS

The combination of clay and boehmite that comprises the simulated corrosion product binds effectively to the aluminum-clad fuel elements. The current drying procedures are adequate to remove the free water from the fuel elements, but these procedures are not adequate for removing all of the chemically bound waters of hydration from corrosion products inside the fuel elements. The drying procedures can produce a consistent level of dryness in the elements, and additional vacuum/heat cycles will not dry the elements further. Only the addition of sufficient heat to achieve temperatures greater than those reached in the drying chamber will provide sufficient energy to break the chemical bonds that retain the remaining waters of hydration.

Examination of plates with wet areas revealed that there is a sharp drying front, which moves towards the center of the plate during drying. The level of wetness does not increase gradually from the outer portion of the plates to the center, rather it changes sharply at the drying front. The drying tests showed that the temperature behavior of the simulated corrosion product on the center plate of an element can indicate when that element is dry.

The thermogravimetric analysis establishes that, in the vast majority of cases, the drying chamber produced a dried simulant that was drier than ambient conditions. In these cases, the weight of the specimen increased while it was exposed to the atmosphere and during the initial stages of heating in the TGA.

ACKNOWLEDGMENTS

REFERENCES

Anderson, P.A., 1995, "Characterization of Corrosion Solids on ATR Fuel Stored in the CPP-603 Basin," PAA-03-95 to C.V. Shelton-Davis, Idaho National Engineering Laboratory, Idaho Falls, Idaho.

Glang, R., 1970, "Vacuum Evaporation," in *Handbook of Thin Film Technology*, eds. L.I. Maissel and R. Glang, McGraw-Hill, New York, pp. 3-37.

Itaya, Y., and M. Hasatani, 1996, "R&D Needs - Drying of Ceramics," *Drying Technology*, 14(6), pp. 1301-1313.

Kasakura, T., and M. Hasatani, 1996, "R&D Needs - Drying of Sludges," *Drying Technology*, 14(6), pp. 1389-1401.

Ketelaars, A.A.J., E.F. Kaasschieter, W.J. Coumans, and P.J.A.M. Kerkhof, 1994, "The Influence of Shrinkage on Drying Behaviour of Clays," *Drying Technology*, 12(7), pp.1561-1574.

Lords, R.E., W.E. Windes, J.C. Crepeau, and R.W. Sidwell, 1996, "Drying Studies of Simulated DOE Aluminum Plate Fuels," *Proc. DOE Spent Nuclear Fuel and Fissile Material Management Meeting*, Reno, Nevada.

Nace, R.L., M. Deutsch, and P.T. Voegli, 1956, *Geography, Geology, and Water Resources of the National Reactor Testing Station, Idaho: Part 2. Geography and Geology*, pp.141-152, U.S. Geological Survey, Boise, Idaho.

van der Zanden, A.J.J., A.M.E. Schoenmakers, and P.J.A.M. Kerkhof, 1996, "Isothermal Vapour and Liquid Transport Inside Clay During Drying," *Drying Technology*, 14(10), pp. 2183-2211.

Wefers, K., and C. Misra, 1987, "Oxides and Hydrides of Aluminum," Alcoa Technical paper, no. 19, Alcoa Laboratories, Aluminum Company of America, Pittsburgh, Pennsylvania.